



SRTTU

Journal of Computational and Applied Research  
in Mechanical Engineering

jcarme.sru.ac.ir

JCARME

ISSN: 2228-7922

## Research paper

# Experimental study on the effect of machining parameters on machining characteristics and surface morphology in ECM

Mohammad Reza Shabgard \* and Reza Rostami Heshmatabad

Department of Mechanical Engineering, University of Tabriz, Tabriz, east Azarbaijan, Iran

## Article info:

### Article history:

Received: 00/00/0000

Revised: 00/00/0000

Accepted: 00/00/0018

Online: 00/00/0000

### Keywords:

Electrochemical machining  
(ECM),

Oxide layer,

Machining characteristics,

Surface morphology,

Surface cavity effect.

### \*Corresponding author:

[mrshabgard@tabrizu.ac.ir](mailto:mrshabgard@tabrizu.ac.ir)

## Abstract

In this study, the relationship between the effect of machining parameters on machining characteristics and surface morphology was studied in electrochemical machining (ECM). The characteristics were material removal rate (MRR), over cut (OC), surface roughness (SR), and surface morphology. The results show that MRR is increased by increasing the current, but OC is decreased. Increasing concentration causes increasing MRR, OC, and SR. Also, the analysis of surface morphology shows that the electrolyte type affects the dissolution mechanism and surface layer formation in ECM. There are cavities in NaCl and KCl; their diameter, depth and distribution on the machined surface are changed by parameters, and their diameters were 4  $\mu\text{m}$  to 9  $\mu\text{m}$ . Increasing ion concentration causes an enhancement in the diameter size and depth of created cavities on the workpiece, but their uniform distribution decreases, while the current has a reverse effect on them. On the other hand, an oxide layer is formed on the machined surface in  $\text{NaNO}_3$ , and by increasing current and concentration, breaking and the anion cavity effect are increased on this layer. So, increasing the MRR and SR is due to this phenomenon in  $\text{NaNO}_3$ .

## 1. Introduction

The ECM process involves controlled anodic dissolution that takes place within the inter-electrode gap, driven by a combination of complex hydrodynamic, chemical, and physical phenomena. These include the transport of ions through the electrolyte, redox reactions occurring at the electrode surfaces, and the convective flow of electrolyte within the electrodes gap [1-5]. The important parameters

of this process are the type and concentration of ions that exist in the machining area, and the electric field that affects the movement rate of ions in this area. Studying the machined surface and residual effects on this surface is important due to the relation between experimental results such as surface roughness (SR), material removal rate (MRR), and over cut (OC). On the other hand, the workpiece surface morphology is an important parameter in the performance and the workpiece time, and it is considered an important characteristic. Some studies had been

done on the effect of input parameters on the output, separately. Tang *et al.* [6] investigated the influence of electrolyte type on the current efficiency and surface roughness. Their result showed that NaCl has the highest current efficiency. Also, when the feed velocity of the cathode increases, a gradual reduction in surface roughness is observed. Sorkhel and Bhattacharyya [7] reviewed parametric control for achieving the optimal quality of the workpiece surface in the ECM process. They used NaCl as an electrolyte in different concentrations. The results showed that the surface smoothness has a directed relationship with the electrolyte flow rate and current density in different concentrations, as well as the electrolyte concentration in a constant current density.

Haisch *et al.* [8] studied the electrochemical dissolution mechanism of 100Cr6 using NaCl and  $\text{NaNO}_3$ . This study indicated that a carbon-rich layer is built up on the bed surface of the sample during machining of 100Cr6 when using a concentrated electrolyte solution of NaCl; this layer has loosely salted boundaries, and it is removed from the workpiece surface by the perturbation of the fluid passing through the specimen. But when  $\text{NaNO}_3$  is used as an electrolyte, a black surface layer forms on the specimen at the anodic potentials to +1.8V rather than the reference electrode NHE, which causes complete passivation of the bed surface of 100Cr6. They observed that forming  $\text{Fe}^{n+}$  increases by increasing current density (anodic potential) and decreasing electrolyte temperature. While in this condition, the oxygen evolution decreases and causes the break of black surface film on the specimen.

Datta and Landolt [9] studied the influence of electrolyte concentration, PH, and temperature on surface brightening of nickel. They used a combination of  $\text{NaNO}_3$  and  $\text{HNO}_3$  electrolytes at different concentrations. The results showed that the current density increases because of more ionization by increasing the electrolyte concentration and temperature, so this case causes the brightening of the workpiece surface. Also, they announced that, in the studied area, the PH of the environment doesn't affect the surface brightening.

It's necessary to study the relationship between the effect of machining parameters on machining characteristics and the residual effects on the machined surface for achieving logical reasons and applying the ECM to real parts. Ions have unique electrochemical properties that have different effects on the dissolution in the ECM. So the purpose of this research is concentrated on the effect of ions (anions and cations) at different concentrations and currents on the machining characteristics, and their relationship with the residual effects on the surface morphology. Therefore, in this study, the main purpose is to focus on this subject for the first time.

## 2. Experimental study

### 2.1. Experimental setup

The electrochemical machining system, as its schematic illustration is shown in Fig. 1, was designed and constructed to do the experiments. This ECM device consists of four units. The voltage of the power supply is between 0 and 12 V, and its maximum current is 200A. The control system includes a number of electronic circuits that can measure and control the gap changes during the machining process. It was innovated, and there are three control methods: the constant current density, defined feeding, and sensing of the workpiece in the specified periods. The constant current density method was used in this study. The tool feeding unit controls the tool moving along the Z axis during the machining process.

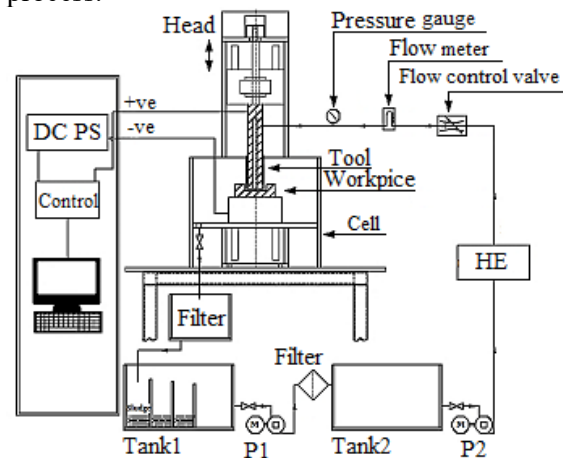


Fig. 1. Schematic illustration of the ECM and its associated equipment.

The electrolyte unit includes storing, feeding, filtering, and temperature control of the electrolyte. There is a filter that is 5  $\mu\text{m}$ , which was used to prevent impurity substances from entering the machining area and make a clean electrolyte in the process. In order to control the temperature of the electrolyte, a thermal exchanger system was used. It includes a 1500W heater, a temperature sensor PT100, a thermostat and current relay. Machining is done in a Plexiglas box, and the workpiece is held by a special fixture in it. Fig. 2 shows the ECM device and equipment related to the performance of experiments.

## 2.2. Experimental Materials

In the current research, commercially available 304 stainless steel was employed as the workpiece material. The elemental makeup of the material was determined using a quantum analyzer, and the weight percentages of its alloying elements are listed in Table 1. Additionally, tools were fabricated from 304 stainless steel, aluminum, and copper. Following preliminary trials, the copper tool was selected for further experiments due to its superior machining performance. Tool wear was found to be negligible. To minimize the effects of stray current and reduce unwanted material dissolution, the lateral surfaces of the tool were insulated with an epoxy coating. Figs. 3 and 4 display the samples and the tool before and after the insulation process, in the given order. In this research, current, electrolyte type, and concentration were considered as key machining parameters. The electrolytes used included NaCl, NaNO<sub>3</sub>, and KCl, which differ in their ionic compositions. NaCl and KCl are categorized as impassive electrolytes, whereas NaNO<sub>3</sub> is classified as a passive electrolyte. These were tested at concentrations of 1, 1.5, and 2 mol/L. Other process parameters — voltage (10V), electrolyte flow rate (3L/min), electrolyte back pressure (0.05 bar G), electrolyte temperature ( $26 \pm 1$  °C), initial inter-electrode gap IEG (0.3 mm), and machining time (5 minutes)—were maintained constant throughout the experiments.



**Fig. 2.** Equipment for experiments: (a) power supply and control unit, (b) transmission and supply of electrolyte fluid unit, and (c) tool feeding unit.

**Table 1.** Weight percent of alloying elements in the 304 stainless steel.

Element	Wt.%	Element	Wt.%
Al	0.024	S	0.018
C	0.046	Si	0.372
Cr	17.670	V	0.069
Cu	0.689	W	0.044
Mn	0.886	Fe	71.360
Mo	0.163	Ni	8.679



**Fig. 3.** Machined workpieces in experiments.

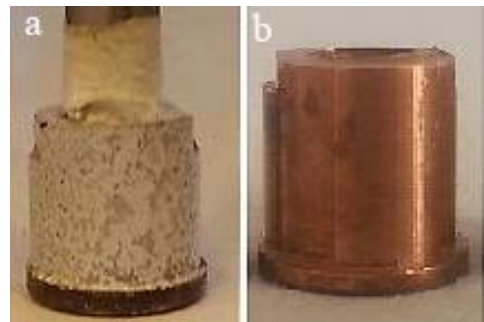


**Fig. 4.** The tool before and after the insulation process: (a) tool after coating and (b) tool before coating.

Table 2 summarizes the ECM experimental conditions. Each experiment was repeated three times, then the average of the experiments was considered the result of each experiment. A standard analytical balance with a precision of 0.0001 g was employed to measure the material removal rate (MRR). Prior to and following the experiments, the samples were thoroughly washed with distilled water, completely dried, and then weighed to determine the mass change. The material removal rate (MRR) was determined using Eq. (1):

$$MRR = \frac{M_1 - M_2}{t} \quad (1)$$

Here, MRR represents the material removal rate (g/min),  $M_1$  is the mass of the workpiece before machining (g),  $M_2$  is the mass after machining (g), and  $t$  is the machining time (min). To measure the OC in the machined samples, a Starrett HS1000 profile projector was utilized. A magnified image of each sample was projected onto the device screen, and several reference points were marked along the side edges of the machined area. The average machined diameter was calculated based on these measurements. The OC value was calculated by Eq. (2):

$$OC = \frac{D_p - D_t}{2} \quad (2)$$

Here,  $D_p$  is the machined workpiece diameter (mm) and  $D_t$  is the tool diameter (mm). The SR of the samples was measured using a Mahr Perthometer roughness tester. Measurements of roughness average ( $R_a$ ) were taken at central, middle, and lateral regions of the workpiece, and the mean of these readings was considered as the SR of the machined workpieces.

### 3. Results and discussion

#### 3.1. Effects of machining parameters on MRR

The MRR variations relative to current in different electrolytes are shown in Fig. 5. As can be seen in Fig. 5, MRR is increased in different electrolytes by increasing the current. The rate of

oxidation and reduction reactions in the machining area are increased by increasing the current, and this raises the stimulation of ions from the workpiece to the electrolyte solution. This phenomenon increases the MRR according to Eq. (3) [6, 10].

$$MRR_g = \eta \frac{AI}{Z.F} \quad (3)$$

**Table 2.** Experimental conditions for ECM.

Parameters	Value	Unit
Voltage	10	V
Current rate	35,45,55	A
Electrolyte flow rate	3±0.5	Lit./min
Back pressure of electrolyte	0.5±0.02	Bar.G
Electrolyte temperature	26±1	°C
Initial setting gap	0.3	mm
Machining time	5	min
Electrolyte type	NaCl, NaNO <sub>3</sub> , KCl	
Electrolyte concentration	1, 1.5, 2	M

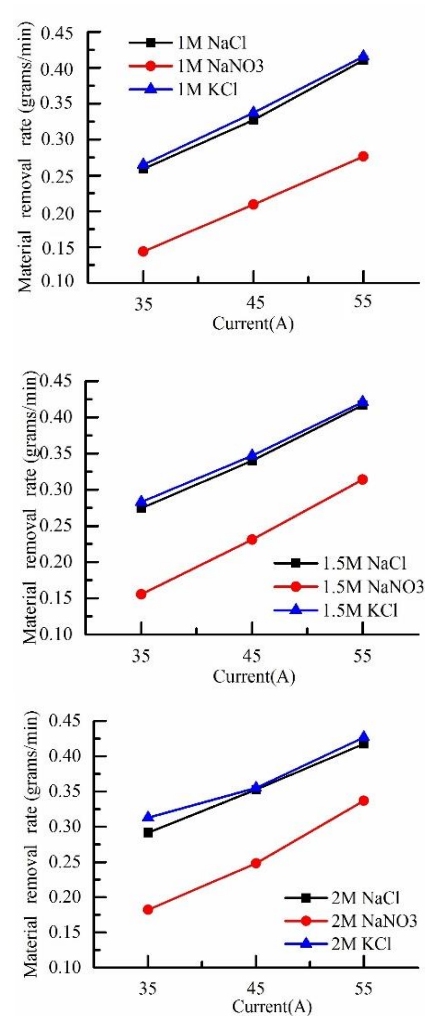


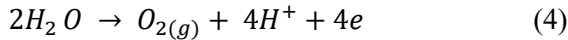
**Fig. 5.** MRR variations relative to the current changes: (a) 1M, (b) 1.5 M, and (c) 2M.



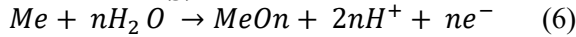
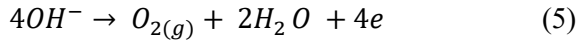
where,  $I$  is the current (A),  $A$  is the atomic mass (g),  $Z$  is the dissolution capacity,  $F$  is the Faraday constant (96500K), and  $\eta$  is the efficiency of the machining current.

Also, as is shown in Fig. 5, the MRR values of  $\text{NaNO}_3$  are less than  $\text{NaCl}$  and  $\text{KCl}$ . This is due to the difference in the participation of  $\text{NO}_3^-$  and  $\text{Cl}^-$  anions in the dissolution process. In machining with  $\text{NaNO}_3$ , part of the machining current, based on Eqs. (4) and (5), is spent for evolution of oxygen and formation of passive layer (oxide layer) on the workpiece surface through Eq. (6). This reduces the efficiency of the machining current and therefore reduces the MRR of  $\text{NaNO}_3$  [6, 8, 11, 12]. But in machining with  $\text{NaCl}$  and  $\text{KCl}$  which have  $\text{Cl}^-$ , the efficiency of the machining current is the maximum due to lack of oxygen evolution and non-formation of the passive layer. This causes to be high rate of machining at these electrolytes compared to the  $\text{NaNO}_3$ , according to Eq. (3) [8].

Acidic environment



Alkaline environment



The MRR variations relative to the molar concentration in different electrolytes are shown in Fig. 6. It can be seen that the MRR is increased by increasing the molar concentration of the electrolyte ion at different currents in all studied electrolytes. The reason can be because of unchanging other parameters of the ECM process; the MRR depends on the value of participation and activity of ions in the dissolution process. By increasing the ions' concentration, the number of ions participating, and their activity are increased. These increase the participation of ions in the dissolution process and therefore increase the MRR [10, 13]. The activity of each ion depends on the ionic strength of the electrolyte ( $I$ ) and it depends on ions' concentration based on Eq. (7) [14, 15].

$$I = 1/2 \sum_{i=1}^n C_i Z_i^2 \quad (7)$$

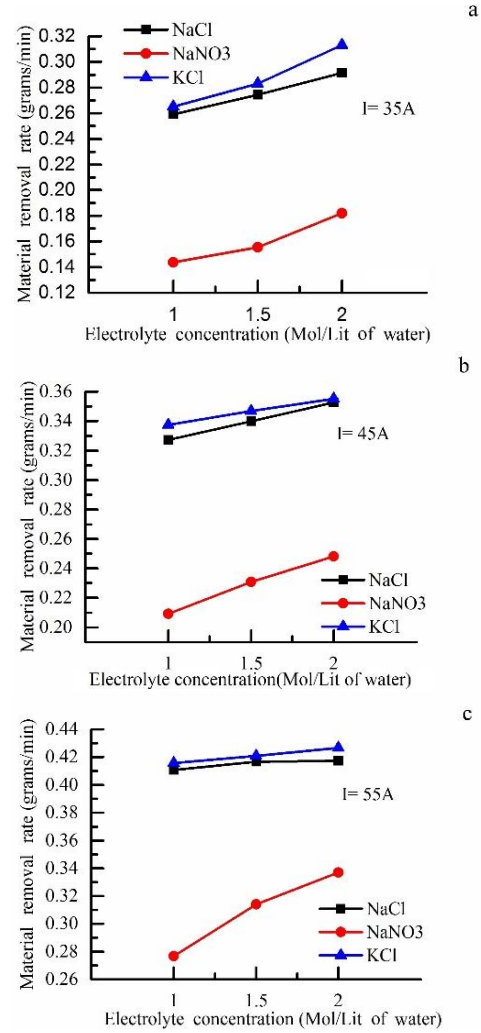


**Fig. 6.** MRR variations relative to the molar concentration in different electrolytes: (a)  $I=35\text{A}$  (b)  $I=45\text{A}$ , and (c)  $I=55\text{A}$ .

where,  $C_i$  is the concentration of ion  $i$ ,  $Z_i$  is the charge number of the ions in the electrolyte solution. Also, it can be seen that the optimal value for all the electrolytes occur in high concentrations. The maximum MRR is 0.4255 g/min, and it was obtained under the machining conditions of electrolyte concentration of 2 molarity and current of 55A with  $\text{KCl}$ .

### 3.2. Effects of machining parameters on OC

The OC variations relative to the molar concentration at different electrolytes are shown in Fig. 7. As can be seen, OC is increased by increasing the molar concentration. The reason is because of the electrolyte molar concentration

on the basis of Eq. (8) that causes to enhance in conductivity of three electrolytes [16]. The high electrolyte conductivity increases the effects of stray current in the side gap area. Therefore, the local effect of electrochemical dissolution reactions decreases in high concentration of ions and causes increasing OC.

$$K = e_0(n_+z_+u_+ + n_-z_-u_-) \quad (8)$$

where, K is the electrolyte conductivity,  $e_0$  is the elementary electric charge,  $n_+$  is the number of cations,  $z_+$  is the charge number of cations,  $u_+$  is the cation mobility,  $n_-$  is the number of anions,  $z_-$  is the charge number of anion and  $u_-$  is the anion mobility.

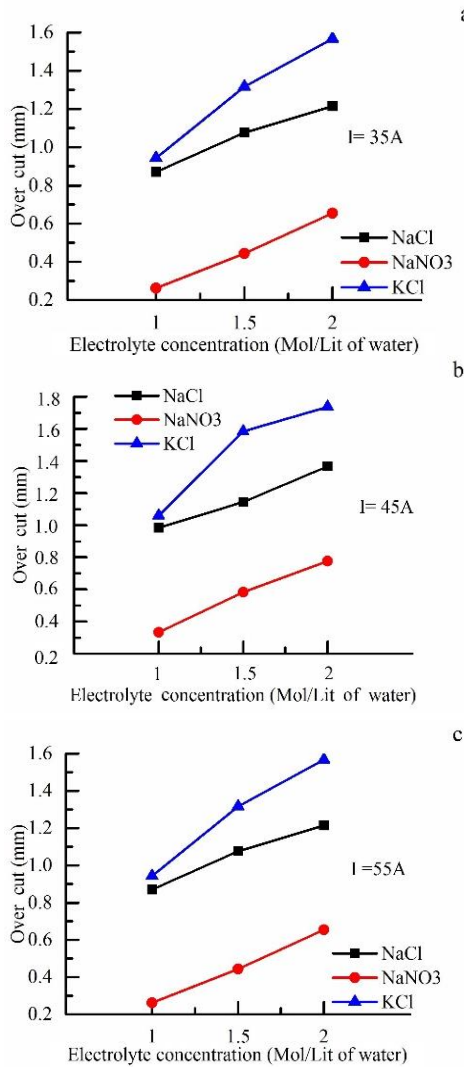


**Fig. 7.** OC variations relative to the molar concentration in different electrolytes: (a)  $I=35A$ , (b)  $I=45A$ , and (c)  $I=55A$ .

It can be seen in Fig. 7, OC values of  $NaNO_3$  are lesser than  $NaCl$  and  $KCl$ . It is due to the passive oxide layer formed on the edge of the workpiece in the machining with  $NaNO_3$ . This reduces the stray current flux in side gap area and, in turn, reduces OC value [17, 18]. Also, Fig. 7 shows that the OC value of  $KCl$  is higher than  $NaCl$ . The high velocity of  $K^+$  compared to  $Na^+$  causes being a difference in the molar conductivity ( $\Lambda$ ) of  $NaCl$  ( $126.45 \text{ cm}^2/\Omega$ ) and  $KCl$  ( $149.85 \text{ cm}^2/\Omega$ ) [16]. The high conductivity of  $KCl$  changes the current density distribution and increases the stray current flux value in the side gap area. This leads to increase the unwanted dissolution value of workpiece so, it increases OC.

The OC variations relative to current are shown in Fig. 8. The OC is reduced by increasing the current in all electrolytes. It is because of by increasing the current, reactions rate increases in the machining gap, so it increases the products of the reactions (metal hydroxides and metal salts) [10]. These products aren't conductive and cause to reduce the value of the stray current flux in the side gap area and OC compared to low currents. The minimum OC obtained in this study is 0.408 mm. It was obtained under the machining conduction of electrolyte concentration of 1 molarity, current of 55A and  $NaNO_3$ .

### 3.3. Effects of machining parameters on SR

The SR variations relative to the current are shown in Fig. 9. According to these results, the SR values of  $NaCl$  and  $KCl$ , in the different concentrations, are reduced by increasing the current, but it is increased by increasing the current in the  $NaNO_3$ . The loose salt layer forms on the surface workpiece in machining with  $NaCl$  and  $KCl$  [3, 19]. It has a direct relation with the amount of current and causes more uniform distribution of the machining current in the workpiece surface at high current densities.

The uniform distribution of machining current in the workpiece surface causes homogeneous dissolution and improves surface smoothness of the workpiece in high current densities. In the  $NaNO_3$ , based on different current, there are three machining zones, passive, transpassive and stable state.

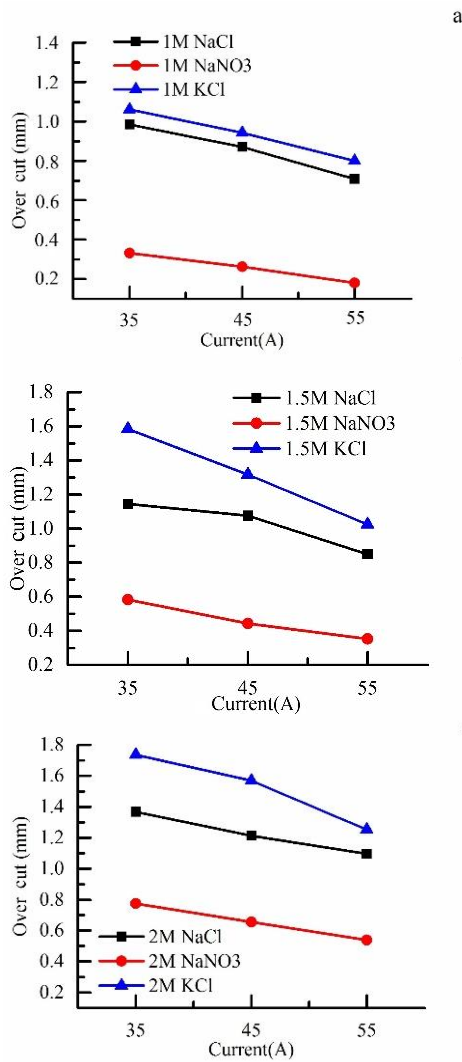


**Fig. 8.** OC variations relative to the current changes in different electrolytes: (a) 1M (b) 1.5 M and (c) 2M.

In the passive zone, the entire current is used for the oxygen gas evolution and formation of the oxide layer. When the current increases, part of the current is used for the breakdown of the oxide layer and this is the transpassive zone. So, the breakdown of the oxide layer increases with increasing of current.

Fig. 10 shows variations of SR compared to the molar concentration. As can be seen, the SR is increased by increasing the electrolyte concentration. It can be stated that by increasing the electrolyte concentration in NaCl and KCl, ion participation is increased in the dissolution process, and it causes increasing the products (metal hydroxides, sludge, and metal salts).

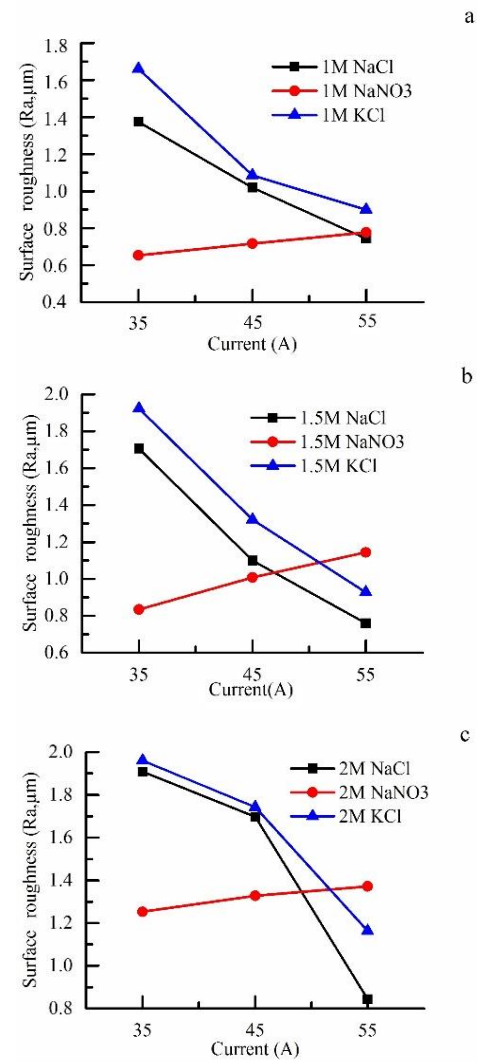


**Fig. 9.** SR variations relative to the current changes in different electrolytes: (a) 1M (b) 1.5 M and (c) 2M.

Therefore, their deposition on the anode surface creates a heterogeneous dissolution and an irregular ECM on the workpiece surface so, SR increases [20]. However, increasing the electrolyte concentration in  $\text{NaNO}_3$  increased the absorbed anions numbers on the oxidized surface. This causes to break the oxide layer and increases the anions cavity effects on this layer, thereby increases SR. According to Fig. 10, it can be seen that at all concentrations and currents, the obtained values of SR for KCl are higher than NaCl. The reason for this difference is high electrical conductivity of KCl compared to NaCl. High mobility of  $\text{K}^+$  increases the rate of electrochemical reactions in the machining area, and it raises heterogeneous dissolution

compared to NaCl. Minimum SR was  $0.465\ \mu\text{m}$ , and it was obtained under the machining conditions of 1 molarity concentration, 55A current and NaCl.

### 3.4. Effects of machining parameters on machined surface morphology

The surface morphology of machined workpiece at concentrations 1, 1.5 and 2 molarity for NaCl and KCl are shown in Figs. 11 and 12. As it is clear in the figures, different morphologies are visible in different concentrations of NaCl and KCl. In these figures, there are some cavities that their diameter, depth, and distribution are changed in the machined surface by changing of electrolyte concentration.

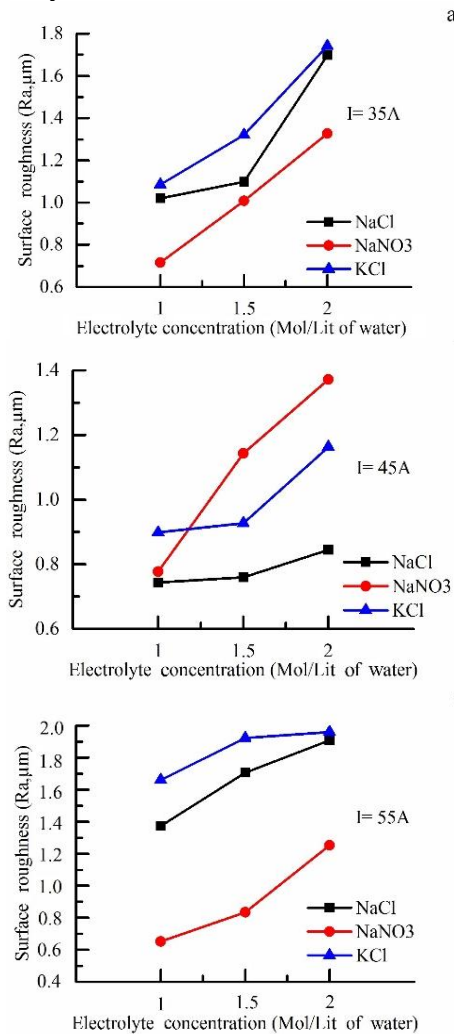


**Fig. 10.** SR variations relative to the electrolyte concentration in different electrolytes: (a)  $I=35\text{A}$ , (b)  $I=45\text{A}$ , and (c)  $I=55\text{A}$ .

The diameter of these cavities is enhanced by increasing concentration, and it is  $4\mu\text{m}$  in 1 molarity,  $7\mu\text{m}$  in 1.5 molarity and  $9\mu\text{m}$  in 2 molarity for both of them. So, this increasing of concentration causes unifying the cavities in some areas and form large cavities, as is shown in Fig. 13, it increases SR. On the other hand, by increasing the concentration, the depth of the cavities is increased, but the uniformity of their distribution is decreased. The effect of electrolyte concentration increasing in the process, which is associated with participation of most ions in the dissolution process, is evident in these figures and that is the creation of heterogeneous machining conditions. The experimental results are according to the results of these figures of machined surface morphology. The surface morphology of the machined workpiece at concentrations 1, 1.5 and 2 molarity of NaNO<sub>3</sub> is shown in Fig. 14.

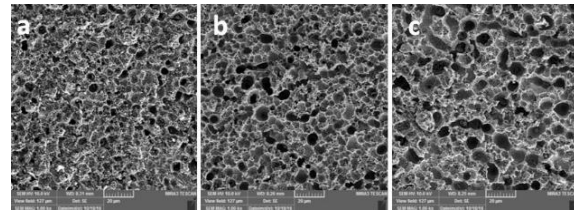


**Fig. 11.** Machined surface morphology in different concentrations of NaCl at 45A current: (a) 1 Molarity, (b) 1.5 Molarity, and (c) 2 Molarity.

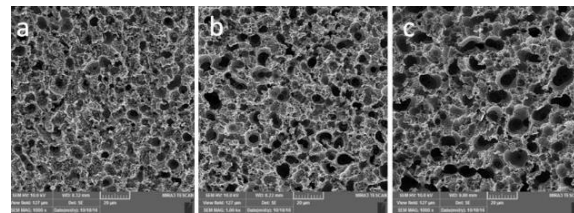


**Fig. 12.** The machined surface morphology in different concentrations of KCl at 45A current: (a) 1 Molarity, (b) 1.5 Molarity, and (c) 2 Molarity.

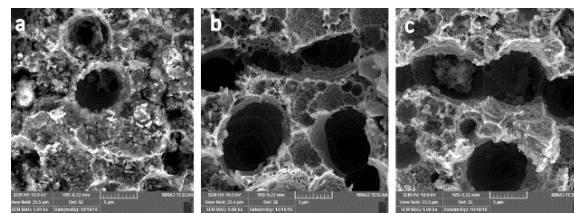


**Fig. 13.** The interference of cavities with each other on machined surface morphology in different concentrations of KCl at 45A current: (a) 1 Molarity, (b) 1.5 Molarity, and (c) 2 Molarity.



In this figure, the oxide layer that is formed in the machining with  $\text{NaNO}_3$ , the breaking and anion cavity effect of this layer are visible clearly. The effect that occurs due to the adhesion of anion to the oxide layer and the creation of cavities and effects on the oxide surface is called the anion cavities effect. It is observed from comparing the panels a, b and c of Fig. 14, the breaking of oxide layer and anion cavity effect on it, are increased by increasing concentration of  $\text{NaNO}_3$ , it is due to high participation of ions in the metal dissolution processes.

By increasing concentration, the more number of  $\text{NO}_3^-$  have a chance to stick on the oxide layer surface and press on it. This phenomenon causes increasing the anion cavity effect and breaking of oxide layer at weak surface areas like the displacements and inclusions. So, according to experimental results and study of the figures of machined surface morphology, it can be stated that by increasing concentration of  $\text{NaNO}_3$ , the surface roughness is increased because of the breaking of oxide layer and anion cavity effect.

Figs. 15 and 16 show the surface morphology of the machined workpiece surface at different currents in 1 molar concentration of  $\text{NaCl}$  and  $\text{KCl}$ . Comparison of panels in the Figs. 15 and 16 shows that by increasing the current of machining, the diameters size and depth of the cavities are reduced greatly and distribution of these cavities is more uniform on the machined surface. So, this indicates by increasing the current, the current distribution on the workpiece surface becomes more uniform and so, as was achieved in experimental results, reduces surface roughness.

Also, Fig. 17 shows the morphology of the machined workpiece surface at different currents in the 1 molarity concentration of  $\text{NaNO}_3$ . The formed oxide layer on the workpiece surface and the anion cavity effect on this layer are shown clearly in panels a, b and c of this figure. According to this figure, by increasing the current, the amount of the breaking of oxide layer and the anion cavity effect on surface of this layer are increased too. Also, the experimental results of section 3. 4 show the surface roughness and machining rate are increased by increasing the current. The effect of

repulsive forces of  $\text{NO}_3^-$  anion, which were attracted on the surface of the oxide layer, is increased by increasing the current, and it causes breaking of the layer at the weak areas. For this reason, the cavities on the surface are enhanced by increasing the current. So, increasing the current in machining with  $\text{NaNO}_3$  causes to break the oxide layer and replace the metal dissolution with the oxygen gas evolution on the workpiece surface.

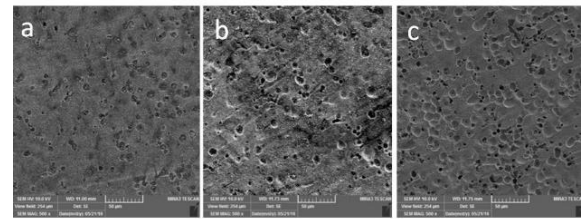


**Fig. 14.** The machined surface morphology in different concentrations of  $\text{NaNO}_3$  at 45A current: (a) 1 Molarity (b) 1.5 Molarity and (c) 2 Molarity.

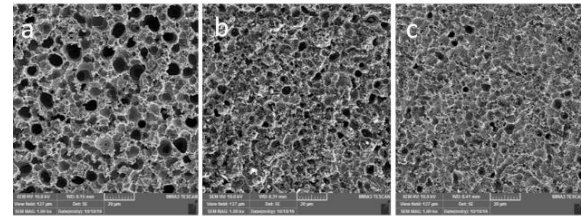


**Fig. 15.** The machined surface morphology at different currents in 1M concentration of  $\text{NaCl}$ : (a) 35A, (b) 45A and (c) 55A.

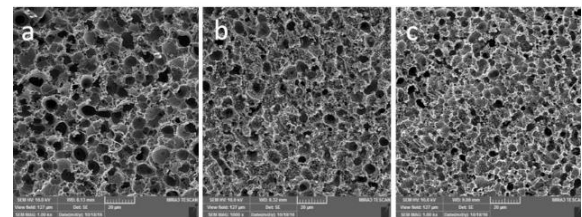


**Fig. 16.** The machined surface morphology at different currents in 1M concentration of  $\text{KCl}$ : (a) 35A, (b) 45A and (c) 55A.

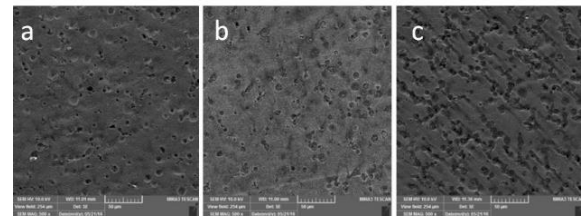


**Fig. 17.** The machined surface morphology at different currents in 1M concentration of  $\text{NaNO}_3$ : (a) 35A, (b) 45A and (c) 55A.

#### 4. Conclusions

In this study, the relationship between effect of machining parameters on the machining characteristics and surface morphology in ECM process were evaluated. The results of this study can be summarized as follows:

1. In ECM of 304 stainless steel, MRR, OC and SR values are increased by increasing the concentration of ions. Also, by increasing the current, MRR is enhanced but OC is decreased.
2. In machining with NaCl and KCl, there are cavities on the machined surface that their diameter, depth, and distribution on this surface depend on the current and concentration of electrolyte ions. But in NaNO<sub>3</sub>, the oxide layer, breaking and cavity effects are observed. Their effects on the machined workpieces surface in two types of electrolytes show the difference in the dissolution mechanism in machining with them.
3. The cavities diameters are increased by increasing the concentration, and their diameters were achieved 4µm in 1M to 9µm in 2M. Also, the depth of cavities is increased by increasing concentration, but their uniform distribution is decreased on the machined surface. In this condition, the surface roughness increased from 1µm in 1M to 1.908µm in 2M. While the current has a reverse effect on them and the surface smoothness improved to 0.65µm.
4. The increasing of concentration and current in NaNO<sub>3</sub> causes to increase the break of oxide layer and the anion cavity effect; so, in this condition SR increases. Also, the current has a greater effect on the break and anion cavity effect of this oxide layer than the concentration.
5. The difference between moving speed of cations Na<sup>+</sup> and K<sup>+</sup> in electrolyte solution caused to change in dissolution and experimental results. The obtained experimental values for MRR, OC and SR in machining with KCl are more than NaCl in the same condition.
6. The optimal parameters for machining 304 stainless steel using the ECM were identified as an MRR of 0.4006 g/min, an OC of 0.7507 mm, and an SR of 0.465 µm, achieved in NaCl with a concentration of 1 M and a current of 55 A.

#### Acknowledgment

The authors express their gratitude to Novin Andish Sahand Co. for its assistance in manufacturing the ECM system and conducting the experiments. Appreciation is also extended to Dr. J. Vallipour for his valuable scientific contributions.

#### References

- [1] M. Sankar, A. Gnanavelbabu, K. Rajkumar and N. A. Thushal, "Electrolytic Concentration Effect on the Abrasive Assisted- Electrochemical Machining of Aluminum-Boron Carbide Composite", *Mater. Manuf. Processes*, Vol.32, pp. 687-692, (2016).
- [2] M. Kalaimathi, G. Venkatachalam, M. Sivakumar, and S. Ayyappan "Experimental investigation on the suitability of ozonated electrolyte in travelling-wire electrochemical machining", *J. Braz. Soc. Mech. Sci.*, Vol. 39, pp. 4589-4599, (2017).
- [3] H. A. G. ElHofy, *Advanced Machining processes*, First ed. McGraw-Hill Education, pp. 8-13 (2005).
- [4] P. S. Pa and H. Hocheng, "Electrochemical Machining" *Advanced Analysis of Nontraditional Machining*, Eds. H. Hocheng and H.V. Tsai, New York. pp. 107-258 (2013).
- [5] E. Rumyantsev and A. Davydov, *Electrochemical machining of metals*, first ed. MIR Publishers, Moscow (1989).
- [6] L. Tang, B. Li, S. Yang et al., "The effect of electrolyte current density on the electrochemical machining S-03 material", *Int J Adv Manuf Technol*, Vol. 71, pp. 1825–1833, (2014).
- [7] S. K. Sorkhel and B. Bhattacharyya, "Parametric control for optimal quality of

- the work piece surface in ECM”, *J. Mater. Process. Technol.* , Vol. 40, pp. 271-286, (1994).
- [8] T. Haisch, E. Mittemeijer and J. W. Schultze, “Electrochemical machining of the steel 100Cr6 in aqueous NaCl and NaNO<sub>3</sub> solutions: microstructure of surface films formed by carbides”, *J. Electrochimica Acta*, Vol. 47, pp. 235–241, (2001).
- [9] M. Datta and D. Landolt, “On the influence of electrolyte concentration, pH and temperature on surface brightening of nickel under ECM conditions”, *J. Appl. Electrochem.* , Vol. 7, pp. 247-252, (1977).
- [10] S. S. Uttarwar and I. K. Chopde, “Study of Influence of Electrochemical Process Parameters on the Material Removal Rate and Surface Roughness of SS AISI 304”, *IJCER*, Vol. 3, No 3, pp. 189-197, (2013).
- [11] D. Wang, Z. Zhu, N. wang, D. Zhu and H. Wang, “Investigation of the electrochemical dissolution behavior of Inconel 718 and 304 stainless steel at low current density in NaNO<sub>3</sub> solution”, *Electrochim. Acta*, Vol. 156, pp. 301-307, (2015).
- [12] D. Wang, Z. Zhu, B. He, Y. Ge and D. Zhu, “Effect of the breakdown time of a passive film on the electrochemical machining of rotating cylindrical electrode in NaNO<sub>3</sub> solution”, *J. Mater. Process. Technol.* , Vol. 239, pp. 251-257, (2017).
- [13] M. V. A. Ramakrishna and S. Venugopal Rao, “Fabrication of ECM and study of its parameters in NaCl electrolyte”, *Mater. Today Proc.* , Vol. 46, Part 1, pp. 934-939, (2021).
- [14] P. Atkins and J. Paula, *Physical Chemistry*, 9<sup>th</sup> ed. W. H. Freeman and Company New York, pp. 190-195, (2010).
- [15] V. S. Bagotsky, *Fundamentals of Electrochemistry*, 2<sup>th</sup>. Ed., Published by Wiley & Sons, Inc., Hoboken, New Jersey, pp. 99-116, (2006).
- [16] M. Robson Wright, *An Introduction to Aqueous Electrolyte Solutions*, Wiley & Sons Ltd., pp. 421-473, (2007).
- [17] H. Hocheng and H. -Y. Tsai, *Advanced Analysis of Nontraditional Machining*, Springer New York Heidelberg Dordrecht London, (2013).
- [18] R. Thanigaivelana, R. M. Arunachalamb, B. Karthikeyanc and P. Loganathan, “Electrochemical micromachining of stainless steel with acidified sodium nitrate electrolyte”, *The 17<sup>th</sup> CIRP Conference on Electro Physical and Chemical Machining (ISEM), Procedia CIRP*, Vol. 6, pp. 351 – 355, (2013).
- [19] M. Datta, “Anodic dissolution of metals at high rates”, *IBM J. Res. Dve.* , Vol. 37, No. 2, pp. 207-226, (1993).
- [20] D. L. Pramanik and A. Chattopadhyay, “Selection of the optimum electrolyte composition and flow rate for machining a particular high alloy steel”, *Precis. Eng.* Vol. 4, No. 1, pp. 44-45, (1982).